In Silico Pharmacology (2018) 6:5
https://doi.org/10.1007/s40203-018-0043-7

ORIGINAL RESEARCH

Computer aided drug design based on 3D-QSAR and molecular docking studies of 5-(1H-indol-5-yl)-1,3,4-thiadiazol-2-amine derivatives as PIM2 inhibitors: a proposal to chemists

Adnane Aouidate[1] · Adib Ghaleb[1] · Mounir Ghamali[1] · Samir Chtita[1] · Abdellah Ousaa[1] · M'barek Choukrad[1] · Abdelouahid Sbai[1] · Mohammed Bouachrine[2] · Tahar Lakhlifi[1]

Received: 14 February 2018 / Accepted: 19 March 2018 / Published online: 28 March 2018

Abstract

PIM2 kinase plays a crucial role in the cell cycle events including survival, proliferation, and differentiation in normal and neoplastic neuronal cells. Thus, it is regarded as an essential target for cancer pharmaceutical. Design of novel 5-(1H-indol-5-yl)-1,3,4-thiadiazol-2-amine derivatives with enhanced PIM2 inhibitory activity. A series of twenty-five PIM2 inhibitors reported in the literature containing 5-(1H-indol-5-yl)-1,3,4-thiadiazol-2-amines scaffold was studied by using two computational techniques, namely, three-dimensional quantitative structure activity relationship (3D-QSAR) and molecular docking. The comparative molecular field analysis (CoMFA) and comparative molecular similarity indexes analysis (CoMSIA) studies were developed using nineteen molecules having pIC_{50} ranging from 8.222 to 4.157. The best generated CoMFA and CoMSIA models exhibit conventional determination coefficients R^2 of 0.91 and 0.90 as well as the Leave One Out cross-validation determination coefficients Q^2 of 0.68 and 0.62, respectively. Moreover, the predictive ability of those models was evaluated by the external validation using a test set of six compounds with predicted determination coefficients R^2_{test} of 0.96 and 0.96, respectively. Besides, y-randomization test was also performed to validate our 3D-QSAR models. The most and the least active compounds were docked into the active site of the protein (PDB ID: **4 × 7q**) to confirm those obtained results from 3D-QSAR models and elucidate the binding mode between this kind of compounds and the PIM2 enzyme. These satisfactory results are not offered help only to understand the binding mode of 5-(1H-indol-5-yl)-1,3,4-thiadiazol series compounds into this kind of targets, but provide information to design new potent PIM2 inhibitors.

Keywords CoMFA · CoMSIA · Molecular docking · PIM2 · Drug design · 5-(1H-indol-5-yl)-1,3,4-thiadiazol

✉ Adnane Aouidate
a.aouidate@hotmail.fr

Adib Ghaleb
adib.ghaleb@gmail.com

Mounir Ghamali
ghamalimounir86@gmail.com

Samir Chtita
samirchtita@gmail.com

Abdellah Ousaa
Abdellahousaa@gmail.com

M'barek Choukrad
mchoukrad@yahoo.fr

Abdelouahid Sbai
sbai.abdelouahid@hotmail.com

Mohammed Bouachrine
bouachrine@gmail.com

Tahar Lakhlifi
tahar.lakhlifi@yahoo.fr

[1] MCNSL, School of Sciences, Moulay Ismail University, Meknes, Morocco

[2] High School of Technology, Moulay Ismail University, Meknes, Morocco

Introduction

The human genome encodes more than 500 Protein kinases receptors (PKs), which is considered one of the largest class of genes in the human body. PIM (Proviral Integration site for Moloney murine leukemia virus) is a subfamily of serine/threonine protein kinases, which are widely expressed and involved in cell survival and proliferation as well as a number of other signal transduction (Nawijn et al. 2011a; Santio et al. 2010). This subfamily is composed of three isoforms: PIM1, PIM2, and PIM3 that share a high-level of sequence homology and exhibit some functional redundancy. Over-expression of PIM1 and PIM2 kinases has been reported in hematologic malignancies also in solid tumors such as diffuse large B cell lymphomas (DLBCL) and prostate cancer (Brault et al. 2010), these findings make them attractive targets for cancer therapy (Nawijn et al. 2011b).

In the literature, several heterocylces as pyrrolo carbazole (Gadewal and Varma 2012), Aminooxadiazole (Wurz et al. 2015) and pyrazines (Qian et al. 2009) have been studied with different approaches so far and found to inhibit the PIM2 and exhibit an anticancer activity. In order to reduce time and coast, to design more potent PIM2 inhibitors, computational research can circumvent these difficulties and allow obtaining precise data while taking advantage of the rapid progress of computing chemical descriptors, which can be obtained easily from publicly available software's. Those can be exploited easily to build quantitative structure activity relationship (QSAR) models to enable calculation of the activity and prediction of the efficacy of newly proposed compounds. For this purpose, a series of some potent PIM2 inhibitors have been designed and reported by Wu et al. (2015), to the best of our knowledge, no 3D-QSAR studies have been carried out based on the reported activities of this series of substituted 5-(1H-indol-5-yl)-1,3,4-thiadiazol-2-amines. That prompted us to aim an in silico study based on this series to extract the structural features to design new molecules with enhanced PIM2 inhibitory activity.

Ligand-based and structure-based are the most widely used approaches in drug discovery and drug design in medicinal chemistry. Structure-based approach includes molecular docking, which is based on the evaluation the interactions between the ligand and binding site of the receptor. While, based-ligand approach, which includes the popular 3-QSAR models, Comparative Molecular Field Analysis (CoMFA) (Kubinyi 2003) and Comparative Molecular Similarity Indexes Analysis (CoMSIA) (Klebe et al. 1994), is based on changes in 3D structures features of molecules such as steric, electrostatic and hydrophobic properties. Indeed, it becomes necessary to develop a QSAR model to predict the biological activity before the synthesis of new PIM2 inhibitors. Whereas, successful 3D-QSAR and molecular docking studies model are not only helps understand relationships between the physicochemical properties and biological activity of any class of molecules, but also provides researchers a deep vision about the lead molecules to be used in further studies to discover new drugs (Gupta et al. 2003).

The present comprises 3D-QSAR (CoMFA and CoMSIA) studies following by docking molecular simulation on a series of twenty-five substituted 5-(1H-indol-5-yl)-1,3,4-thiadiazol-2-amine derivatives (Hong et al. 2012) to identify the required key structural features to design and optimize new leads able to inhibit the PIM2 kinase. We think that the findings extracted from this current study might be beneficial to design highly potent PIM2 inhibitors.

Materials and methods

Data collection

For molecular docking and 3D-QSAR studies a set of twenty-five compounds with their reported IC_{50} values for inhibition of PIM2 activity were taken from literature (Wu et al. 2015). For the QSAR analysis in vitro biological activities IC_{50} (μM) were converted into the corresponding pIC_{50} values (i.e. pIC_{50} is the negative logarithm of IC_{50} ($pIC_{50} = -\log(IC_{50})$) and are listed with their corresponding structures in Fig. 1 and Table 1, the dataset was split into two sets nineteen molecules were chosen randomly to build the quantitative model (training set) and the remaining molecules were used to test the performance of the proposed model (Test set).

Molecular modeling

All modeling studies were performed using the SYBYL-X 2.0 molecular modeling package (Tripos Inc., St. Louis, USA) running on a windows 7, 32 bits workstation. Three-dimensional structures of the studied compounds were built using the SKETCH option in SYBYL, then they were

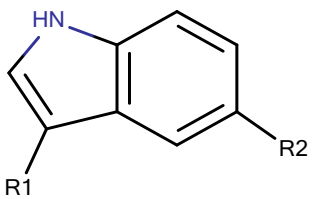

Fig. 1 The chemical structure of the 5-(1H-indol-5-yl)-1,3,4-thiadiazol-2-amine derivatives

Table 1 Chemical structures and anti-cancer activities of substituted 5-(1H-indol-5-yl)-1,3,4-thiadiazol-2-amines derivatives

No	R_1	R_2	pIC_{50}	No	R_1	R_2	pIC_{50}
1*	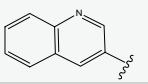	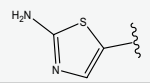	5.567	14	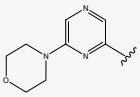	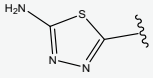	7.921
2	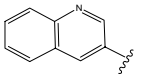	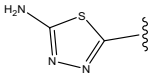	5.996	15	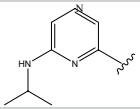	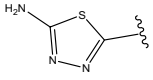	8.000
3	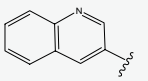	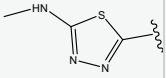	5.788	16	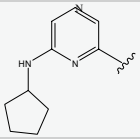	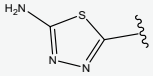	8.222
4	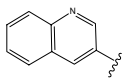	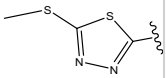	4.658	17	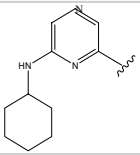	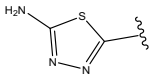	7.745
5	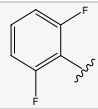	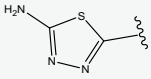	6.458	18*	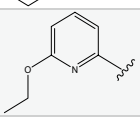	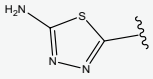	7.658
6	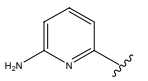	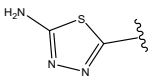	6.010	19*	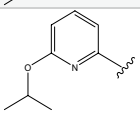	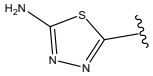	8.000
7	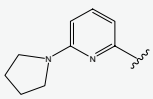	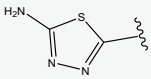	6.983	20*	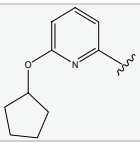	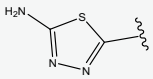	7.387
8*	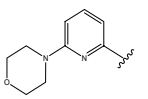	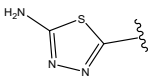	7.229	21	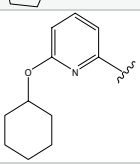	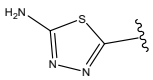	6.943
9	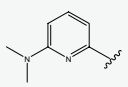	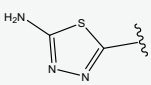	7.432	22	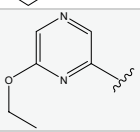	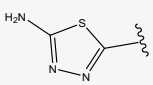	7.553
10	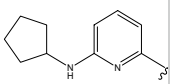	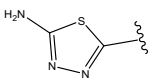	7.678	23	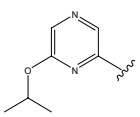	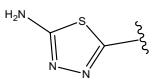	7.770
11*			6.644	24			7.602
12			6.717	25			5.889
13			7.377				

* Test set

minimized under the Tripos standard force field (Clark et al. 1989) with Gasteiger–Hückel atomic partial charges (Purcell and Singer 1967) by the Powell method with a convergence criterion of 0.01 kcal/mol Å.

Molecular alignment

Molecular alignment is a vital step in the development of any 3D-QSAR study (AbdulHameed et al. 2008). The Fig. 2 depicts the proposed alignment, all molecules were aligned on the common core of 5-(1H-indol-5-yl)-1,3,4-thiadiazol-2-amine by distil alignment technique available in SYBYL. The best-docked conformation of compound **16** is chosen to align the dataset in 3D-QSAR studies and serve as a template molecule to visualize the contour maps.

CoMFA studies

The Comparative Molecular Fields Analysis (CoMFA) was performed to evaluate steric and electrostatic energies of the Tripos force fields implemented in SYBYL-X 2.0. All the analyses were performed in a 3D regularly spaced grid of 2.0 Å in all Cartesians directions, a sp^3 carbon with a Van Der Waals radius of 1.52 Å and net + 1.0 charge was used as a probe, which was placed at each lattice point of the grid box to generate respectively, the steric (Lennard-Jones potential) and electrostatic (Coulomb potential) fields. The default cut-off energy value was set at 30 kcal/mol for both steric and electrostatic fields (Ståhle and Wold 1988).

CoMSIA studies

The Comparative Molecular Similarity indexes Analysis (CoMSIA) (Klebe et al. 1994) model was carried out on SYBYL-X 2.0, using the same training and test sets, and the same grid box as used in CoMFA calculation. Five fields (Electrostatic, steric, hydrophobic, Hydrogen bond donor and acceptor) were calculated from similar actives molecules, to develop the CoMSIA model. A sp^3 carbon with a charge, hydrophobic interaction, and Hydrogen bond donor and acceptor properties of + 1.0 was used as a probe at every grid point to measure the five above-mentioned fields. In the present study, the value of attenuation factor, which controls the Gaussian function's steepness, was set by default at 0.3 (Zheng et al. 2011).

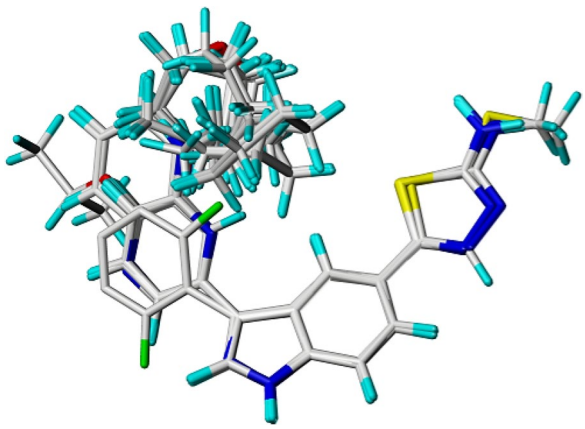

Fig. 2 3D-QSAR structure superposition and alignment (**a**) of training and test sets using molecule 16 as a template

Partial least square (PLS) analysis

Because of the enormous variables obtained from the fields' calculations, the PLS regression method (Wold 1991), is generally performed to evaluate a linear correlation between the CoMFA, CoMSIA fields and the biological activity values. In the first step, the cross (Q^2) validation was performed by using leave-one-out (LOO) (Kubinyi 2003) method where one compound is eliminated from the training set and its activity is predicted from the developed model using the residual compounds. The same way is repeated until all compounds have been eliminated once. The highest value of Q^2 with the lowest cross-validation standard error of estimate (S_{cv}) and a minimal number of components was accepted. In order to reduce noise and increase the speed up the analytical process, the column filtering value (σ) was set to 2.0 kcal/mol. In the next step and after getting the optimum number of components, they were used to derive the final PLS model with no validation method (Baroni et al. 1992; Cruciani et al. 1992) to obtain the maximum determination coefficient (R^2).

Validation and predictive power of the model

The main objective of any QSAR study is to obtain a model with the highest predictive and generalization abilities. So to evaluate the predictive power of the developed 3D-QSAR models, six compounds were used as a testing set (Golbraikh and Tropsha 2002). These molecules were aligned using the same methods described above, then their inhibitory activities were predicted using the generated CoMFA and CoMSIA models from the training set.

Y-Randomization test

The obtained models were further validated by the Y-Randomization method (Rücker et al. 2007). The activities of the studied molecules (pIC_{50}) are randomly shuffled many times and after every iteration, a new QSAR model is developed. The new QSAR models are expected to have lower Q^2 and R^2 values than those the original models. This technique is performed to eliminate the possibility of the chance correlation. If higher values of the Q^2 and R^2 are obtained, it means that an acceptable 3D-QSAR can't be generated for

this data set because of the structural redundancy and chance correlation.

Model acceptability criteria

According to Alexander Tropsha and Alexander Golbraikh, a predictive model must satisfy a set of statistical criteria. A QSAR model was considered predictive if the following conditions are satisfied (i) $Q^2 > 0.50$; (ii) $R^2 > 0.60$ (Golbraikh and Tropsha 2002; Tropsha et al. 2003).

Docking

To validate the obtained results from CoMFA and CoMSIA contour maps, molecular docking study was performed using Surflex-dock implemented in SYBYL-X.2.0. The ligands and protein preparation steps for the docking protocol were carried out in SYBYL-X 2.0, then results were analyzed using Discovery Studio (2016) and MOLCAD ([CSL STYLE ERROR: reference with no printed form.]) programs.

Macromolecule preparation

The crystal structure of PIM2 was downloaded from the Protein Data Bank, (PDB entry code: **4 × 7q**). No one of the understudy ligands is complexed with this protein in PDB, so, its original ligand was removed then the most and least active compounds from our data set were docked into the active site of the studied protein. The PDB file was prepared using Discovery Studio 2016, such as all ligands, cofactors and solvent molecules were removed from the model.

Ligand preparation

The selected compounds for docking were modeled in the same way as for the 3D-QSAR studies, Three-dimensional structures were built using the SKETCH option in SYBYL, then they were minimized under the Tripos standard force field (Clark et al. 1989) with Gasteiger–Hückel atomic partial charges (Purcell and Singer 1967) by the Powell method with a convergence criterion of 0.01 kcal/mol Å.

Molecular surface physicochemical properties (MOLCAD)

MOLCAD is a module in SYBYL, which is used to visualize interactions between the ligand and protein. The fast Connolly method was used to generate surface physicochemical maps of the integrase binding site using properties, namely, electrostatic potential, hydrophobic potential, and Hydrogen bonding potential. These generated surface property maps are generally complementary to CoMFA and CoMSIA contour maps.

Results and discussion

The predicted and experimental activity values and their residual values for both the training and test sets from CoMFA and CoMSIA models are given in Table 2.

CoMFA results

Based on CoMFA descriptor available on SYBYL, a 3D-QSAR model was proposed to explain and predict quantitatively the steric and electrostatic fields effects of substituents on the anti-cancer activity of a series of twenty-five substituted 5-(1H-indol-5-yl)-1,3,4-thiadiazol-2-amines.

As discussed earlier distil alignment method was used in the present study, the obtained statistical keys for the CoMFA model, as Q^2, R^2, R^2_{test}, F-t, and S_{cv} were determined by SYBYL are shown in Table 3.

A Q^2 value higher than 0.5 is considered significant for the chance of significant correlation being < 95%. For the

Table 2 Experimental and calculated anti-cancer activity (pIC_{50}) of compounds in the training set and the test set for the final CoMFA and CoMSIA models

No	pIC_{50} (obs)	PIC_{50} (pred)			
		CoMFA	Residu	CoMSIA	Residu
1	5.5670	5.683	− 0.1163	5.613	0.1322
2	5.9960	5.748	0.2473	5.827	0.2531
3	5.7880	5.215	0.5728	5.609	0.2036
4	4.6576	5.058	− 0.4004	4.976	0.0951
5	6.4584	6.455	0.0034	6.468	0.0165
6	6.0101	6.386	− 0.3761	6.152	0.1056
7	6.9830	7.040	− 0.0573	7.053	0.1872
8	7.2291	7.173	0.0558	7.703	0.2386
9*	7.4318	7.468	− 0.0357	7.550	0.0936
10	7.6778	7.695	− 0.0170	7.661	0.3177
11	6.6440	7.209	− 0.5651	7.003	0.4229
12	6.7167	6.812	− 0.0948	6.678	0.3145
13	7.3768	7.446	− 0.0693	7.553	0.2569
14*	7.9208	7.535	0.3858	8.197	0.0054
15*	8.0000	7.910	0.0898	7.810	0.3577
16	8.2218	8.011	0.2108	8.221	0.3456
17	7.7447	7.589	0.1559	7.597	0.1338
18	7.6576	7.420	0.2377	6.905	0.5045
19	8.0000	7.687	0.3128	7.495	0.4678
20	7.3870	7.084	0.3034	7.217	0.0134
21	6.9430	6.948	− 0.0047	7.193	0.4462
22	7.5530	7.797	− 0.2441	7.435	0.0848
23	7.7700	7.924	− 0.1547	8.020	0.2461
24*	7.6021	7.406	0.1960	7.809	0.3180
25*	5.8894	5.817	0.0722	5.936	0.7801

Table 3 PLS Statistics of CoMFA and CoMSIA models

Model	Q^2	R^2	S_{cv}	F-t	N	R^2_{test}	Fractions				
							Ster	Elec	Acc	Don	Hyd
CoMFA	0.68	0.91	0.310	39.267	4	0.96	0.896	0.104	–	–	–
CoMSIA	0.62	0.90	0.325	35.363	4	0.96	0.385	0.093	0.244	–	0.277

Q^2 Cross-validated determination coefficient, N Optimum number of components obtained from cross-validated PLS analysis and same used in final non-cross-validated analysis, R^2 Non-cross-validated determination coefficient, S_{cv}: Standard error of the estimate, F-t F -test value, R^2_{test}: External validation determination coefficient

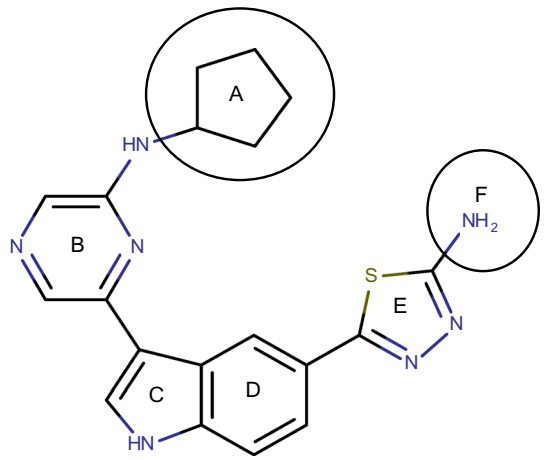

Fig. 3 The structure of the most active molecule (**16**) used in the contour analyses

selected CoMFA model, the cross-validated determination coefficient Q^2 value of the training set and non-cross-validated determination coefficient R^2 are 0.68 and 0.91 respectively. The optimal number of principal components using to generate the CoMFA model is four, which is reasonable regarding the number of molecules used to build the model. The standard error is 0.310. Finally, the prediction ability of the proposed model was confirmed using the external validation, the R^2_{test} value obtained is 0.96. Those statistics results indicated the good stability and the powerful predictive ability of CoMFA model.

CoMSIA results

Based on CoMSIA descriptor available on SYBYL, a 3D-QSAR model was proposed to explain and predict quantitatively, the hydrophobic, electrostatic, steric, donor and acceptor fields effects of substituents on the anti-cancer activity of a series of twenty-five substituted 5-(1H-indol-5-yl)-1,3,4-thiadiazol-2-amines.

Different combinations of the five fields were generated. The best CoMSIA proposed model contains just four fields (Electrostatic, steric, hydrophobic, and acceptor). The cross-validated determination coefficient Q^2 value of the training set and non-cross-validated determination coefficient R^2 are 0.62 and 0.90 respectively. The optimal number of principal components using to generate the CoMSIA model is four, which is reasonable considering the number of molecules used to build the model. The standard error is 0.325. Finally, the prediction ability of the proposed model was confirmed using the external validation, the R^2_{test} value obtained is 0.96. Those statistics results indicated the good stability and the powerful predictive ability of proposed CoMSIA model.

Contour analysis

3D-QSAR contour maps were generated to visualize the data contents of the derived CoMFA and CoMSIA models, which provide the information about the favorable and unfavorable regions for the biological activity in the studied compounds. Changes in the structure of the molecule lead to changes in its physico-chemical properties, which might increase or decrease the biological activity. The CoMFA steric and electrostatic contour maps are shown in Fig. 4. Steric, electrostatic, hydrophobic and Hydrogen bond acceptor contour maps of CoMSIA are shown in Fig. 5. Compound **16** is the most active of the series; therefore it was taken as reference structure for the generation of contour maps (Fig. 3).

CoMFA contour map

CoMFA steric and electrostatic contours are displayed in Fig. 4a, b. The steric interactions are denoted by green and yellow contours, while the electrostatic interactions are denoted by the red and blue contours. The fractions of the steric and electrostatic fields were 89.6% and 10.4% respectively.

The most active molecule in the series (Molecule **16**) is displayed superimposed with CoMFA steric and electrostatic contour maps in Fig. 4a, b respectively. In the CoMFA steric contour map Fig. 4a, a large green contour map is located over of the A region, suggests that inhibitors with bulky groups at this position should be more active than those with no or smaller groups. In case of compounds as **10** ($pIC_{50} = 7.678$) and **20** ($pIC_{50} = 7.387$), which are sterically favorable due to the presence of the N-cyclopenthylamino

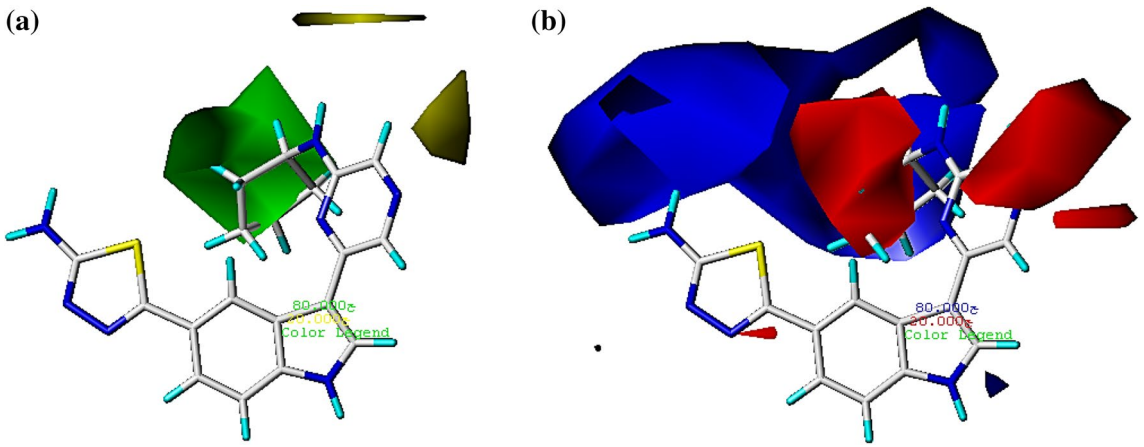

Fig. 4 **a**, **b** Std* coeff. contour maps of CoMFA analysis with 2 Å grid spacing in combination with compound 16. **a** Steric fields: green contours (80% contribution) indicate regions where bulky groups increase activity, while yellow contours (20% contribution) indicate regions where bulky groups decrease activity. **b** Electrostatic fields: blue contours (80% contribution) indicate regions where electron-donating groups increase activity, while red contours (20% contribution) indicate regions where electron-withdrawing groups increase activity

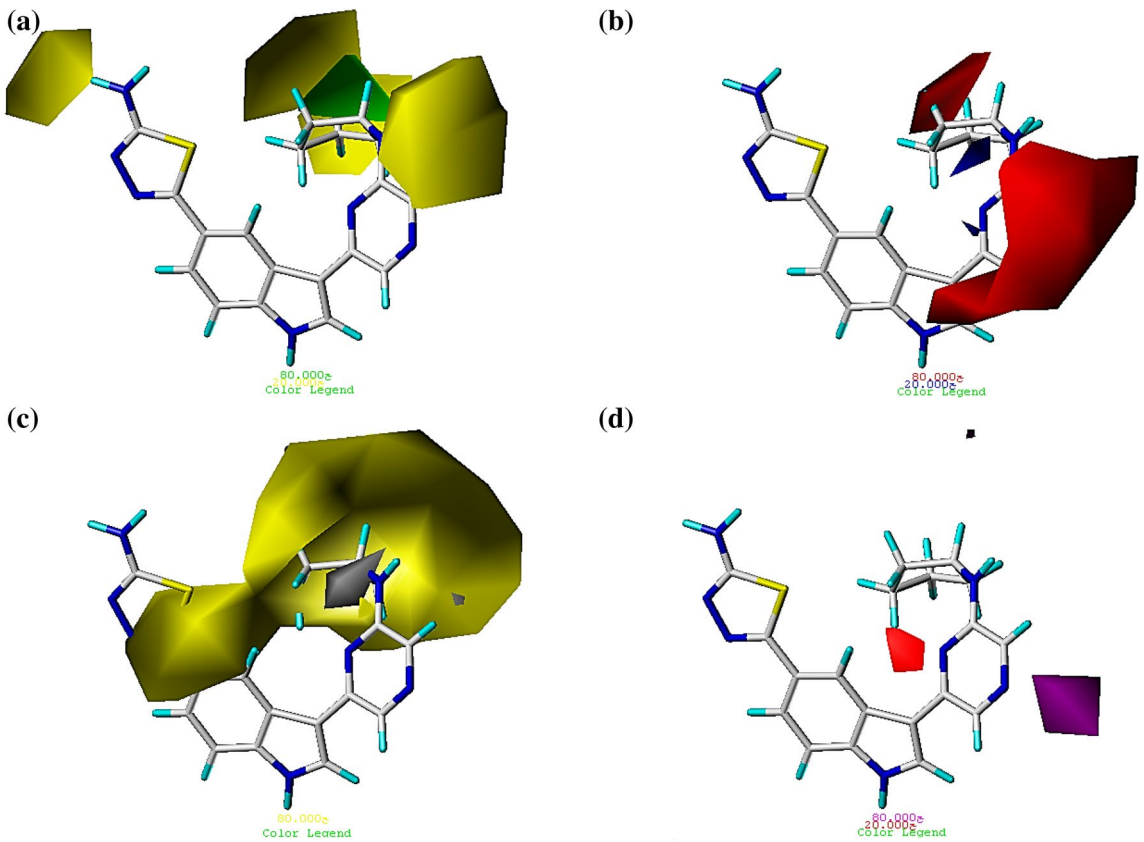

Fig. 5 Std* coeff. contour maps of CoMSIA analysis with 2 Å grid spacing in combination with compound 16. **a** Steric contour map: green contours (80% contribution) indicate regions where bulky groups increase activity, while yellow contours (20% contribution) indicate regions where bulky groups decrease activity. **b** Electrostatic contour map: red contours refer to regions where electron-donating groups are favored while blue contours indicate regions where electron-withdrawing groups are favored. **c** Hydrophobic contour map. Yellow contours (80% contribution) indicate regions where hydrophobic substituents are favored, gray contours (20% contribution) refer to regions where hydrophilic substituents are favored (**d**) Hydrogen-bond acceptor contour map. The magenta contours (80% contribution) for Hydrogen-bond acceptor groups increase activity; red contours (20% contribution) indicate the disfavored region

and cylopentoxy on A region, were more potent than **6** ($pIC_{50}=6.010$) where it was absent, which lead into decrease of activity. Around the 4 and 5 positions of B ring, it's located two yellow maps indicating that small groups are favorable to the inhibitory activity. That fact compounds **1** ($pIC_{50}=5.567$) with a benzene ring linked to the B ring and **26** ($pIC_{50}=5.889$) with a isopropoxy at 4 position show less potency than other compounds without substituents at those positions. In the CoMFA electrostatic contour maps Fig. 4b, a blue color indicates that substituents should be electron deficient for high binding affinity towards the receptor-binding site and a red contour indicates that substituents should be electron rich for high binding affinity. A red contour map is located over the A region, suggests that electronegative groups at this position will increase the inhibitory activity. This may explain why the activity of compound **19** with an isopropoxy ($pIC_{50}=8.000$) is greater than of **18** with an ethoxy ($pIC_{50}=7.658$). A blue contour map is located on, and between A and F regions, indicates that any electropositive group at this position would increase the anti-cancer activity. Another one is located near to B ring, which suggests that electropositive groups at this position will increase the inhibitory activity. Further, increasing electronic density at this position will bring sown the activity, this may explain the less activities of compounds **3** ($pIC_{50}=5.788$) and **4** ($pIC_{50}=4.658$), that have electronegative substituents which fell in the unfavorable blue areas and thus exhibit low PIM2 inhibitory activity.

These contour maps provide us some general insight into the nature of the receptor-ligand binding region.

In the CoMSIA model, the steric and electrostatic contour maps Fig. 4a, b are more or less similar to those of CoMFA model discussed above and they highlight almost the same information. Therefore, our following discussion will focus on the hydrophobic and Hydrogen bond acceptor fields. The fractions of the steric, electrostatic, hydrophobic and Hydrogen bond acceptor fields were 38.5, 9.3, 24.4 and 27.7% respectively.

In the hydrophilic contour maps depicted in Fig. 4c, it is shown a yellow area located between the A and E rings and another large one located on the A region, which suggest that these moieties are contributing to the lipophilicity. Thus, it is suggesting that increase in the lipophilicity in these regions expected to improve the PIM2 inhibitory activity. While a gray contour map is covering the NH groupe between to the A region and B ring in compound **16** indicationg that hydrophilic substituents are preferred in this region. Significanly, compound **23** ($pIC_{50}=7.770$) with an isopropyl substituent at the A region, and an –O group between the A region and B ring, which are directely fallen in the yellow and the gray contours respectivelly, showed higher activity than the corresponding compound **5** ($pIC_{50}=6.458$), which has a lipophilic Fluro substituent near the gray area between the A region and B ring.

The magenta contour maps Fig. 4d indicate the areas where Hydrogen bond accepting groups increased activity and red contour maps indicate areas where Hydrogen bond accepting groups decreased activity. A magenta contour located near the right nitrogen atom of the pyrazine moiety (B ring) suggests the requirement of Hydrogen bond accepting groups at this position to enhance the inhibitory activity. While a red contour located near the left nitrogen atom of the pyrazine (B ring) suggests that the presence of Hydrogen bond accepting groups at this position will lead to decrease the PIM2 inhibitory activity. This is due to the fact that the pyridine ring is more basic than the pyrazine, so the presence of another nitrogen atom on the B ring decreases its Hydrogen acceptor ability.

Furthermore, a pyridine ring at the B ring, a hydrophobic and moderate group in term of steric bulk at the A region as an cyclopentyl substituted by Fluor atom or methyl group may lead to increase in the PIM2 inhibitory activity of the molecule. As well as this observation was in agreement with the steric contour map in CoMFA model.

Outliers

To check the outliers in the proposed 3D-QSAR models, we considered empirically that inhibitors with a residual between predicted and experimental pIC_{50} values above one logarithm unit considered as outliers and should be removed. According to these rules, any compound neither in training set nor in test set was regarded as outlier.

External validation

Validation of the developed model is an essential part of any QSAR study. Thus, a true and trustworthy model should be able to predict a precise activity in the external test set (Golbraikh and Tropsha 2002). That is why the final developed CoMFA and CoMSIA models from a training set of nineteen 5-(1H-indol-5-yl)-1,3,4-thiadiazol-2-amine derivatives were used to predict the activity of 5 remaining molecules, The parameters of the performance of the generated models are shown in Table 3.

Y-Randomization

The Y-Randomization method was carried out to validate the CoMFA and CoMSIA models. Several random shuffles of the dependent variable were performed then after every shuffle, a 3D-QSAR was developed and the obtained results are shown in Table 4. The low Q^2 and R^2 values obtained after every shuffle indicate that the good result in our original

Table 4 Q^2 and R^2 values after several Y-randomization tests

Iteration	CoMFA		CoMSIA	
	Q^2	R^2	Q^2	R^2
1	− 0.066	0.92	0.031	0.80
2	− 0.122	0.90	0.095	0.86
3	0.095	0.90	0.079	0.88
4	− 0.444	0.95	− 0.264	0.94
5	− 0.106	0.67	− 0.160	0.57
6	0.036	0.94	− 0.522	0.79
7	0.017	0.89	− 0.105	0.71

CoMFA and CoMSIA models are not due to a chance correlation of the training set.

Docking results

Since the crystal structure of the human PIM2 protein (PDB ID: **4xq7**) is known, Surflex-Dock was applied to investigate the binding mode between these indoles and PIM2 receptor as well as to better understand and support the in vitro activity of the studied compounds for the rational design of drugs (Fig. 6).

In the present work, the most and the least active compounds were selected for further detailed analysis to evaluate the binding mode of this series of 5-(1H-indol-5-yl)-1,3,4-thiadiazol-2-amine derivatives into the active site of PIM2 receptor and results were shown in Fig. 7. The MOLCAD surface of active site within compound **16** was also displayed with cavity depth (CD) Fig. 8a, Hydrogen bond site (HB) Fig. 8 (b), electrostatic potential (EP) Fig. 8c, and lipophilic potential (LP) Fig. 8d, to further explore the interaction between these inhibitors and the receptor. Furthermore, these potentials on a protein surface can be used to find the sites that act attractively on ligands by matching opposite colors (Table 5).

Compound **16** was taken for explanation, as it could be seen from Figs. 7a, b and 8, the cyclopantyl substituent of the A region is making hydrophobic contact with Leu 38 and it shows some far van deer Waals interactions with Gly 39 and Lys 40 indicated that bulky groups were steric favorable in this direction,. As discussed in sections of CoMFA and CoMSIA results, two yellow contour maps over the B ring indicated that bulky groups were steric unfavorable in this direction as steric clash might occur. Which is proven by molecular docking results, such as the pyrazinic ring was observed near the cavity formed by amino acids Phe 43 and Glu 167. Those results are in concordance with the CoMFA and CoMSIA results for steric interactions shown in Figs. 4a and 5a respectively, which suggested that appropriately bulky groups had favorable steric interactions at the A region.

As can be seen in Figs. 7a, b and 8b, compound **16** shows two Hydrogen bond interactions with the protein receptor, which are also supported by Surflex results. The first one is formed between the –NH- of the thiadiazol moiety and the Glu 117 amino acid in the hinge region, which indicated the necessity of the –H atom at this position for high inhibitory activity (NH–O–, distance, 2.66 Å). The pyrridyl ring of the indole moiety exhibited one other Hydrogen bond with Glu 83 amino acid at distance 2.88 Å. Furthermore, the magenta contour map from CoMSIA model is fallen in a region close to the Asp 182, which is considered a Hydrogen bond acceptor. Thus, obtained results from docking and QSAR models are harmonious.

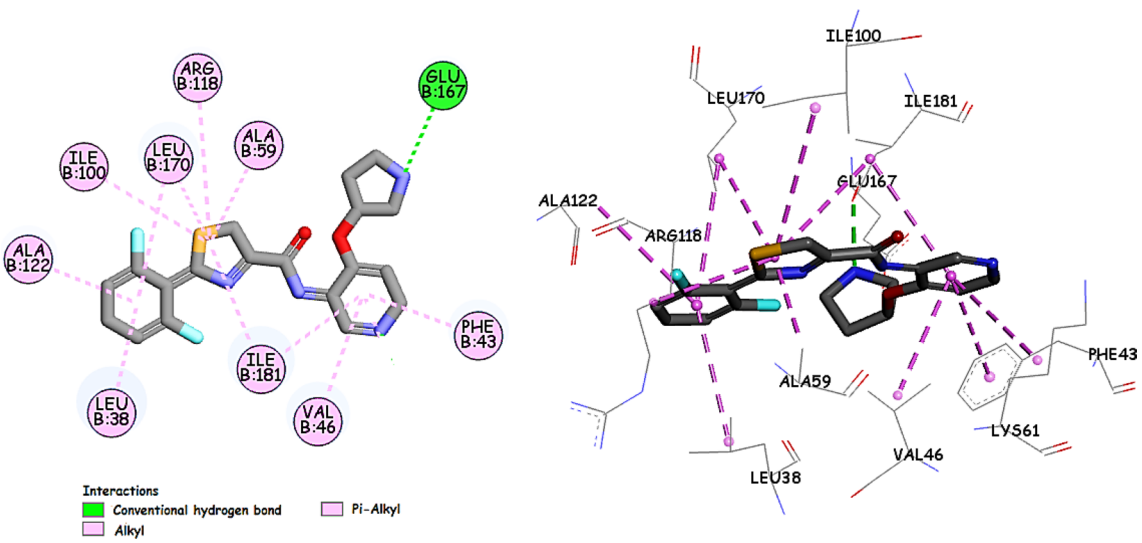

Fig. 6 Binding mode of original ligand

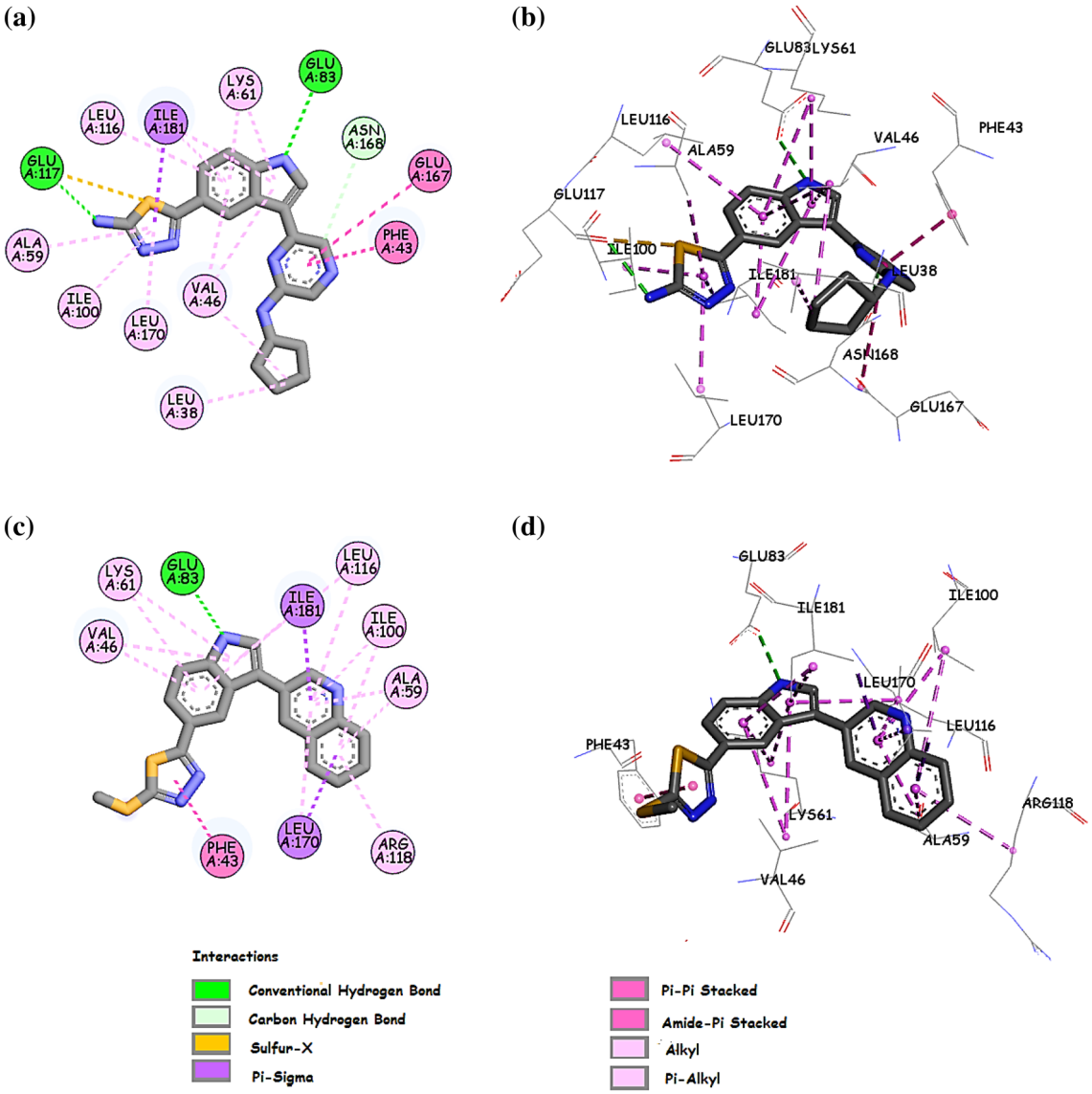

Fig. 7 The binding conformations and ligand interactions of the most and least active inhibitors at the active site of PIM2. **a** and **b** 2D and 3D binding pose view of compound **16**, (**c** and **d**) 2D and 3D binding pose view of compound **4**

In Figs. 7a, b and 8c, the A region and B ring were found next to yellow and cyan areas, which indicated that electron-donating properties at this site were essential for the potency, since the electronegative amino acids (Phe 43) is around there, and its benzene ring forms a Pi–Pi stacked interaction with B ring of the ligand. Where the part between the F and A regions are anchored in a blue area, which suggested that electron-withdrawing substituent at this position would be favored., in addition to a Pi-alkyl interaction bond with Lys 61. The observations obtained from this electrostatic potential surface satisfactorily matched the corresponding CoMFA and CoMSIA electrostatic contour maps.

In Fig. 7a, b and 8d, the cyclopentyl of the A region and the thiadiazol of the E ring were oriented to the solvent area, suggesting that a hydrophobic substituents would benefit the PIM2 inhibitory; the observations satisfactorily matched those of the CoMSIA hydrophobic contour map.

By comparison, the interactions that the best and worst ligands do with the proteins it found that the difference in activity between compounds **16** and **4** might be attributed to their flexibility behaviors; Compound **4** may not reach the hinge region Glu 117 because of its rigid behavior. Whereas compound **16** is more flexible that allows it to reach the hinge region and interacts by Hydrogen bond with Glu 117 and other hydrophobic interactions with different residues, by following a similar binding pattern as with the medication **HBI** compound in PIM2 (PDB ID: **2iwi**) (Bullock et al. 2009), it also appeared to form other Hydrogen bond with

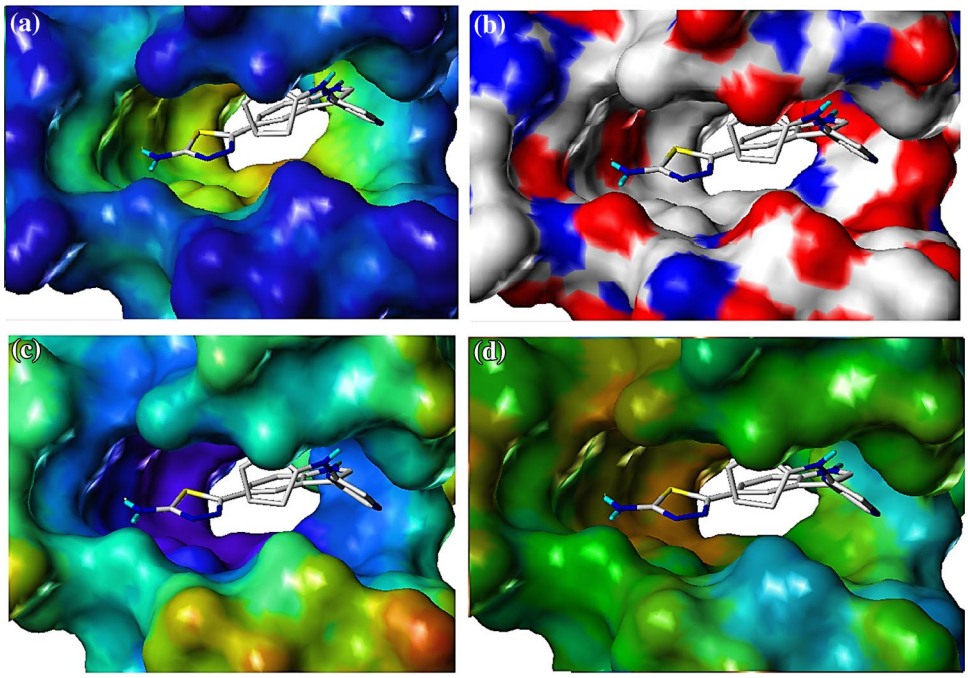

Fig. 8 3D view of the binding conformation and ligand interaction of the most active inhibitor at the active site of PIM2. **a** MOLCAD generated cavity depth potential surface map [(Blue, low depth values = outside of the pocket) (Light red, high depth values = cavities deep inside the pocket).]. **b** MOLCAD generated H-bond potential surface map of the PIM2 active site (Red, H-bond acceptor; blue, H-bond donor). **c** MOLCAD generated electrostatic potential surface map of the PIM2 active site [(Blue, negative potential; red/brown, positive potential). **d** MOLCAD generated lipophilicity potential surface map of the PIM2 active site (Brown, hydrophobic; blue, hydrophilic]

Table 5 The molecular interactions between the most active compound and PIM2 protein

Interaction type	Inhibitor indole 16	Inhibitor indole 4
Hydrogen bonds	Glu 83 and Glu 117	Glu 83
carbon Hydrogen bond	Leu 38	
Pi-Sigma	Ile 181	Leu 170, Ile 181
Pi-Alkyl	Val 46 Ala 59, Lys 61, Ile 100, leu 116 and Leu 170	Val 46, Ala 59, Lys 61, Ile 100, Leu 116 and Arg 118
Pi–Pi stacked and Amid-Pi stacked	Phe 43 and Glu 167	Phe43

Table 6 Properties of compounds **16**

Property	Com 16	Comp 4
Log P	2.91	4.53
H-bond acceptor	4	3
H-bond donor	4	1
Polar surface area (A^2)	107.86	108.00
No. of atoms	27	24
Rotatable bonds	4	3
Molecular weight (g/mol)	375.49	374.48
IC_{50} (PIM2) µM	0.006 Wu et al. (2015)	> 22 Wu et al. (2015)

other residues that what may explain the good inhibitory activity of this compound.

After the molecular docking, and the analysis of the various properties of compounds **16** and **4** in Table 6, it can be concluded that they fulfills the Lipinski's rule (Lipinski 2004) and they could be optimized to give more potent compounds, while the main cause of the mediated PIM2 inhibition of compound **16** is due to its flexible behavior, which allows it to fit the ATP binding site and permits it to make hydrophobic interactions with different hydrophobic residues and with the hinge region of the receptor (Fig. 9).

Design for new PIM2 inhibitors

Overall, this study can be used for the designing of novel PIM2 inhibitors, so, based on the obtained structural requirements from the proposed 3D-QSAR (CoMFA/CoMSIA) models and molecular docking simulation. Three new substituted 5-(1H-indol-5-yl)-1,3,4-thiadiazol-2-amines analogues have been designed to enhance the inhibitory activity. The newly predicted structure ***Indol1*** showed higher inhibitory activity (pIC_{50} = 8.072 and 8.491 for CoMFA and CoMSIA models respectively) than that of the most active compound of the series.

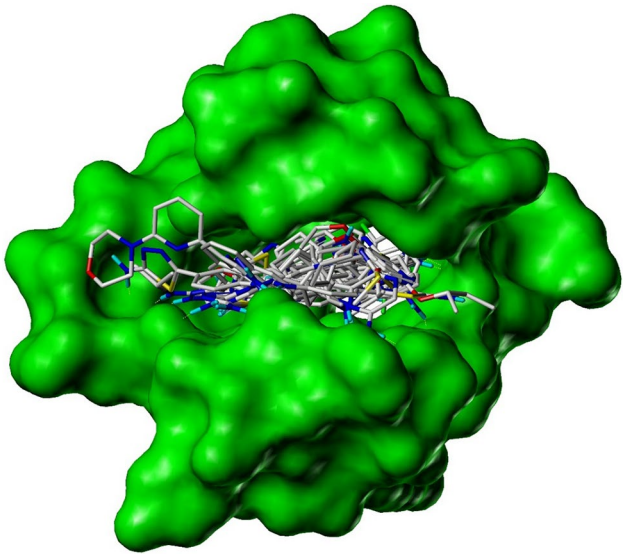

Fig. 9 The MOLCAD surface of the active site within the training and test sets aligned by docking study

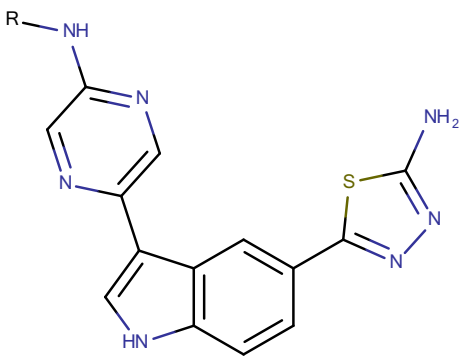

These newly designed molecules were aligned to the database using compound **16** as template and their theoretical pIC_{50} values were predicted by the above proposed models. The predicted PIM2 inhibitory activity of the newly designed molecules was found to be quite similar based on both CoMFA and CoMSIA models.

The docking of the proposed molecule ***Indol1*** as depicted in Fig. 10 reveals that it follows a similar binding mode as the most active compound in the series, such as it keeps the same conformation at the binding pocket of PIM2, and it shows a sulfur-x interaction with Glu 117, and Pi-Alkyl interaction with Lys 61, while the steric bulk caused by the CH3 group at the A region makes the Hydrogen of the NH group between A region and B ring near the Glu 167 amino acid, thus the proposed structure is stabilized by three Hydrogen bonds instead two in compound **16**. Moreover, the newly designed molecules were analyzed for their various properties and results shown that they follow the Lipinski's rule of five for oral bioavailability. ***Indol1*** has the highest predicted activity and it exhibits similar interactions as the most active molecule in the series

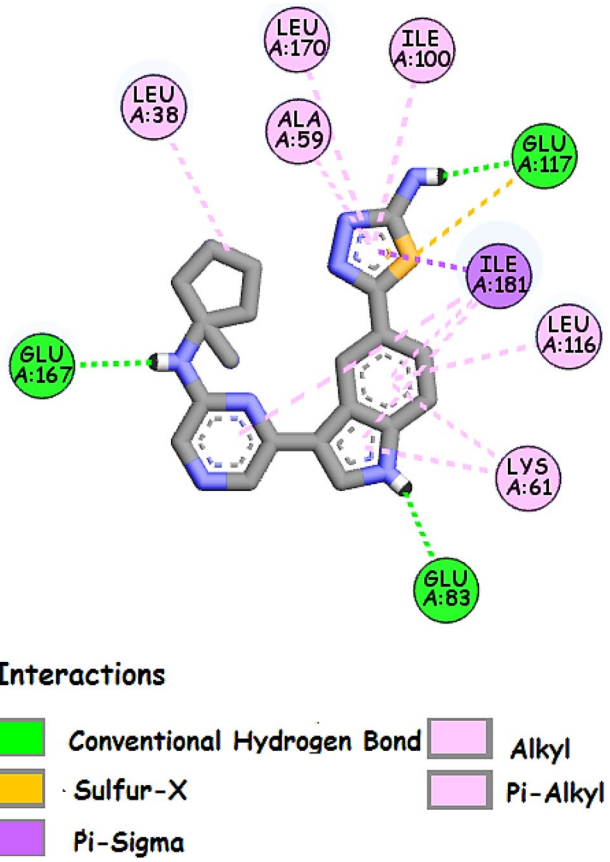

Fig. 10 2D view of the binding conformations and ligand interactions of the proposed ***Indol1*** inhibitor at the active site of PIM2

(Compound **16**) as shown in Fig. 8, a Hydrogen bond with Glu 167, which was found in the original ligand co-crystallized with the **4** × **q7** and it is considered vital interaction for the PIM2 inhibition. Therefore is regarded to be as lead candidate. Chemical structures and predicted pIC_{50} values for those newly designed molecules against the PIM2 along with their Log P, H-bond acceptor (H-A), H-bond donor (H–D), Polar surface area (P.S) (A^2), Rotatable Bonds (R.B), Molecular weight (MW) (g/mol) and energy of affinity (EA) (kcal/mol) (conditions of Lipinski's "rule of five") are given in Table 7.

Conclusion

In this research, both ligand-based and structure-based analyses were conducted based on twenty-five 5-(1H-indol-5-yl)-1,3,4-thiadiazol-2-amine derivatives, not only to generate highly statistical and predictive capabilities 3D-QSAR models, but in order to explore the interaction mechanism between this class of molecules and the PIM2 protein, also identify the key structural features required to design new potent inhibitors. The best CoMFA ($Q^2 = 0.68$, $R^2 = 0.98$) and CoMSIA ($Q^2 = 0.62$, $R^2 = 0.98$) models displayed

Table 7 Structures and chemical properties of newly designed molecules and their predicted pIC_{50} based on CoMFA and CoMSIA 3D-QSAR models

No	Structure	Predicted pIC_{50} (μM)		Log P	H-A	H-D	P.S	R.B	MW
		CoMFA	CoMSIA						
Indo1	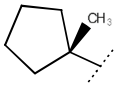	8.072	8.491	3.16	6	4	133.64	4	391.49
Indo2	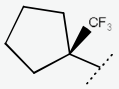	8.040	8.458	3.88	6	4	133.64	5	445.46
Indo3	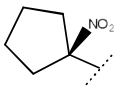	8.052	8.372	1.89	11	4	179.46	5	422.46

satisfactory results in term of several rigorous statistical keys, such as Q^2 and R^2_{test}, for both the internal and external data sets. Hence, molecular docking simulation was used to better understand the binding mechanism and produce the binding poses of these compounds into PIM2 enzyme; in addition to complete, those obtained results from 3D-QSAR studies. Further, all those outcomes showed insight into the key structural features required for the PIM2 inhibitory behavior in the studied 5-(1H-indol-5-yl)-1,3,4-thiadiazol-2-amine derivatives: the compound should be built around the indole core, which must bear F region capable of forming a Hydrogen bond with Glu 117, and a moiety adequate to create hydrophobic interactions with Lys 61 and to give Hydrogen bonding to Glu 83, besides to a steric substituent on the A region able to make the NH between the B ring and the A region more closer to be attracted by the Glu 167 amino acid in order to form a Hydrogen bond.

Thus, those obtained results were used to design novel molecules, which might be proved as potent PIM2 inhibitors. The predicted PIM2 inhibitory activity of the proposed molecules was found to be quite similar based on both CoMFA and CoMSIA models.

Acknowledgment We are grateful to the "Association Marocaine des Chimistes Théoriciens" (AMCT) and "Moroccan centre of scientific and technique research" (CNRST) for their pertinent help concerning the programs.

Compliance with ethical standards

Competing interests The authors declare that they have no competing interests.

References

AbdulHameed MDM, Hamza A, Liu J, Zhan C-G (2008) Combined 3D-QSAR modeling and molecular docking study on indolinone derivatives as inhibitors of 3-phosphoinositide-dependent protein kinase-1. J Chem Inf Model 48(9):1760–1772. https://doi.org/10.1021/ci800147v

Baroni M, Clementi S, Cruciani G, Costantino G, Oberrauch D, Riganelli E (1992) Predictive ability of regression models. Part II: selection of the best predictive PLS model. J Chemom 6:347–356

Brault L, Gasser C, Bracher F, Huber K, Knapp S, Schwaller J (2010) PIM serine/threonine kinases in the pathogenesis and therapy of hematologic malignancies and solid cancers. Haematologica [Internet] 95(6):1004–1015. Available from: http://www.haematologica.org/cgi/doi/10.3324/haematol.2009.017079

Bullock AN, Russo S, Amos A, Pagano N, Bregman H, Debreczeni JÉ et al (2009) Crystal structure of the PIM2 kinase in complex with an organoruthenium inhibitor. Gay N, editor. PLoS ONE 4(10):e7112. https://doi.org/10.1371/journal.pone.0007112

Clark M, Cramer RD, Van Opdenbosch N (1989) Validation of the general purpose tripos 5.2 force field. J Comput Chem [Internet] 10(8):982–1012. Available from: http://www.ncbi.nlm.nih.gov/pubmed/12192139

Cruciani G, Baroni M, Clementi S, Costantino G, Riganelli D, Skagerberg B (1992) Predictive ability of regression models. Part I: standard deviation of prediction errors (SDEP). J Chemom 6(6):335–346. https://doi.org/10.1002/cem.1180060604

Dassault Systèmes BIOVIA, Discovery Studio Modeling Environment, Release 2017, San Diego: Dassault Systèmes. [Internet]. [cited 2017 Feb 25]. Available from: http://accelrys.com/products/collaborative-science/biovia-discovery-studio/

Gadewal N, Varma A (2012) Targeting Pim-1 kinase for potential drug-development. Int J Comput Biol Drug Des 5(2):137–151

Golbraikh A, Tropsha A (2002) Beware of q^2! J. Mol. Graph. Model [Internet] 20(4):269–76. Available from: http://www.ncbi.nlm.nih.gov/pubmed/11858635

Gupta SP, Mathur AN, Nagappa AN, Kumar D, Kumaran S (2003) A quantitative structure-activity relationship study on a novel class of calcium-entry blockers: 1-[(4-(aminoalkoxy)phenyl)sulphonyl] indolizines. Eur J Med Chem [Internet]. 38(10):867–73. Available from: http://www.ncbi.nlm.nih.gov/pubmed/14575933

Hong S, Kim J, Seo JH, Jung KH, Hong SS, Hong S (2012) Design, synthesis, and evaluation of 3,5-disubstituted 7-azaindoles as Trk inhibitors with anticancer and antiangiogenic activities. J Med Chem 55(11):5337–5349. https://doi.org/10.1021/jm3002982

Klebe G, Abraham U, Mietzner T (1994) Molecular similarity indices in a comparative analysis (CoMSIA) of drug molecules to correlate and predict their biological activity. J Med Chem 37(24):4130–4146. https://doi.org/10.1021/jm00050a010

Kubinyi H (2003) Comparative molecular field analysis (CoMFA). Handb Chemoinformatics. https://doi.org/10.1002/9783527618279.ch44d

Lipinski CA (2004) Lead- and drug-like compounds: the rule-of-five revolution. Drug Discov Today Technol 1(4):337–41. Available from: http://linkinghub.elsevier.com/retrieve/pii/S1740674904000551

Nawijn MC, Alendar A, Berns A (2011a) For better or for worse: the role of Pim oncogenes in tumorigenesis. Nat Rev Cancer Nature Publishing Group 11(1):23–34. Available from: http://www.nature.com/nrc/journal/v11/n1/pdf/nrc2986.pdf%5Cnhttp://www.ncbi.nlm.nih.gov/pubmed/21150935

Nawijn MC, Alendar A, Berns A (2011b) For better or for worse: the role of Pim oncogenes in tumorigenesis. Nat Rev Cancer 11(1):23–34. https://doi.org/10.1038/nrc2986

Purcell WP, Singer JA (1967) A brief review and table of semiempirical parameters used in the Hueckel molecular orbital method. J Chem Eng Data 12(2):235–246. https://doi.org/10.1021/je60033a020

Qian K, Lian W, Cywin CL, Farmer BT, Hickey E, Homon C et al (2009) Hit to lead account of the discovery of a new class of inhibitors of pim kinases and crystallographic studies revealing an unusual kinase binding mode. J Med Chem 52(7):1814–1827

Rücker C, Rücker G, Meringer M (2007) Y-randomization and its variants in QSPR/QSAR. J Chem Inf Model 47(6):2345–2357

Santio NM, Vahakoski RL, Rainio E-M, Sandholm JA, Virtanen SS, Prudhomme M et al (2010) Pim-selective inhibitor DHPCC-9 reveals Pim kinases as potent stimulators of cancer cell migration and invasion. Mol Cancer 9(1):279. https://doi.org/10.1186/1476-4598-9-279

Ståhle L, Wold S (1988) Multivariate data analysis and experimental design in biomedical research. Prog Med Chem 25:291–338. Available from: http://www.ncbi.nlm.nih.gov/pubmed/3076969

SYBYL-X 2.0 [Internet]. St. Louis, MO, USA: Tripos Inc; Available from: http://www.tripos.com

Tropsha A, Gramatica P, Gombar VK (2003) The importance of being earnest: validation is the absolute essential for successful application and interpretation of QSPR models. QSAR Comb Sci 22(1):69–77

Wold S (1991) Validation of QSAR's. Quant Struct Relatsh 10(3):191–193. https://doi.org/10.1002/qsar.19910100302

Wu B, Wang HL, Cee VJ, Lanman BA, Nixey T, Pettus L et al (2015) Discovery of 5-(1H-indol-5-yl)-1,3,4-thiadiazol-2-amines as potent PIM inhibitors. Bioorganic Med Chem Lett 25(4):775–780. https://doi.org/10.1016/j.bmcl.2014.12.091

Wurz RP, Pettus LH, Jackson C, Wu B, Wang HL, Herberich B et al (2015) The discovery and optimization of aminooxadiazoles as potent Pim kinase inhibitors. Bioorganic Med Chem Lett 25(4):847–855. https://doi.org/10.1016/j.bmcl.2014.12.067

Zheng J, Xiao G, Guo J, Zheng Y, Gao H, Zhao S et al (2011) Exploring QSARs for 5-Lipoxygenase (5-LO) Inhibitory Activity of 2-Substituted 5-Hydroxyindole-3-Carboxylates by CoMFA and CoMSIA. Chem Biol Drug Des 78(2):314–321. https://doi.org/10.1111/j.1747-0285.2011.01146.x